Macromolecules 1992, *25*, 4948–4954

Chain and Sphere Diffusion in Polyisobutylene–$CHCl_3$: A Reanalysis[†]

George D. J. Phillies*

Department of Physics, Worcester Polytechnic Institute, Worcester, Massachusetts 01609

Wyn Brown and Pu Zhou

Institute of Physical Chemistry, Box 532, 751 21 Uppsala, Sweden

Received February 11, 1992; Revised Manuscript Received May 27, 1992

ABSTRACT: Previously reported (Brown, W.; Zhou, P. *Macromolecules* **1989**, *22*, 4031; Zhou, P.; Brown, W. *Macromolecules* **1989**, *22*, 890) experimental studies of diffusion in polyisobutylene (PIB)–$CHCl_3$ are reconsidered, comparing diffusion coefficients D_p and D_{ch} of silica spheres and random-coil polymers in PIB–$CHCl_3$ solutions. In solutions of low-molecular-mass matrix polymers, D_p/D_{ch} is virtually independent of matrix concentration c; a rapidly-relaxing matrix is equally effective at retarding polymer chains and rigid spheres. On the other hand, in solutions of high-M polymers, with increasing c D_{ch} falls far more rapidly than D_p; large-M chains are far more effective at retarding chains than at retarding spheres of the same size. These results are consistent with the hydrodynamic scaling model but are inconsistent with models that grant to polymer chains an additional diffusive mode inaccessible to rigid spheres. D_p in PIB–$CHCl_3$ follows accurately the universal scaling equation $D_p/D_0 = \exp(-\alpha(cM^{\gamma})^{\nu})$.

I. Introduction

The elucidation of the nature of chain dynamics in nondilute polymer solutions remains a major problem of physical chemistry. It was at one time widely believed that tube-type pictures—de Gennes' reptation model[1] and the Doi–Edwards[2] treatment—gave a qualitatively adequate picture of polymer dynamics, as witnessed by apparent observation of scaling laws $D_{ch} \sim P^{-2}$ and $D_{ch} \sim c^{-1.75}$ for the self-diffusion coefficient D_{ch} of chains at concentration c having molecular mass P.[5] This belief was usually subject to the caveat that a discrepancy existed between predicted ($\eta_m \sim P^3$) and observed ($\eta_m \sim P^{3.4}$) molecular mass dependences of melt viscosity η_m.

It has more recently become apparent that support for tube models from solution measurements and computer simulations is at best ambiguous. [Melts, a separate issue, are not considered here.] One of us (G.P.) argued[3,4] from an extensive survey of the experimental literature that "reptation is probably not important for polymer self-diffusion in solution". Similarly, Lodge et al.[6] concluded a thorough recent review "it is unlikely that reptation is significant in the semidilute regime" though "in entangled melts [reptation] is often the dominant mode". After extensive computer studies, Grest and Kremer[7] found that simulations gave strong evidence for reptation, but Skolnick et al.[8] found that chain self-diffusion is dominated by transverse rather than longitudinal ("reptational") motion.

A variety of alternative models for the dynamics of polymer fluids exist. In addition to reptation/static entanglement treatments,[1,2,9] one also finds dynamic entanglement,[8] hydrodynamic/renormalization group,[10] coupled relaxation,[11] and hydrodynamic scaling[4] models. These models differ as to the relative importance assigned to different interpolymer forces (excluded volume, hydrodynamic) and as to the appropriate approximations and mathematical methods to be used in dynamics calculations. The relative validity of these models, not all of which are mutually exclusive, is presently in dispute.

One way to test models of chain dynamics is to examine how polymer architecture affects diffusion. In general, a diffusion experiment measures the motion of one species (the "probe") through a background solution, which may contain a substantial concentration of dissolved ("background" or "matrix") polymers. For example, tube-type models generally predict that a concentrated solution of linear polymers can be far more effective at retarding the diffusion of star or ring polymers than at retarding the diffusion of linear chains. Stars are predicted to diffuse far more slowly than linear chains if the data are scaled to equal arm length, while the opposite is true in comparing star and linear chains having equal total molecular mass. Wheeler et al.[12,13] measurements on diffusion of linear and star polystyrenes through poly(vinyl methyl ether)–*o*-fluorotoluene are consistent with this prediction, though one may argue[14] that some other models are also consistent with Wheeler et al.'s[12,13] findings.

This paper presents an alternative test of the effect of probe architecture on diffusion in polymer solutions. Here we compare diffusion of random-coil chains and of rigid spherical probe particles through solutions of a linear polymer, namely, polyisobutylene (PIB). Unlike previous comparisons of random-coil and globular probes,[14,15] both probes diffused through the same matrix polymer solution, so that no uncertainties arise from a variation between the chain and globular probe studies in the identity of the matrix. Comparison is made between PIB–$CHCl_3$ data and the systems studied previously.

The measurements of chain and sphere diffusion in PIB–$CHCl_3$ were reported previously;[16–18] these references supply experimental details. In summary, the globular probes were sterically-stabilized silica spheres with radii of 1595 and 318 Å, while the random-coil probes were linear polyisobutylenes; the matrix chains were also linear polyisobutylenes. Diffusion coefficients were measured by quasi-elastic light scattering (QELS). Scattering by the highly dilute silica spheres dominated the spectra of sphere–PIB mixtures; a small PIB spectral component was eliminated by using a maximum-entropy constrained Laplace inversion method.[19,20] For PIB probes in a PIB–$CHCl_3$ matrix solution, both the dilute probes and the potentially more concentrated matrix polymers contrib-

---

* To whom correspondence should be addressed; phillies@wpi.wpi.edu.

[†] The partial support of this work by the National Science Foundation under Grant DMR 91-15639 is gratefully acknowledged.

0024-9297/92/2225-4948$03.00/0

Table I
Nonlinear Least-Squares Fits of D_{ch}/D_0 of Silica Spheres in PIB–CHCl$_3$ to Equation 3 for Data Exhibited in Figure 1[a]

D_{ch}/D_0	α	γ	ν	% rmse	D_{ch}/D_0	α	γ	ν	% rmse
(1.0)	0.33	(0.55)	0.753	17.2	(1.0)	0.332	(0.55)	0.75	18
(1.0)	0.161	(0.55)	(1.0)	40	(1.0)	0.164	(0.55)	(1.0)	40
(1.0)	0.360	0.584	0.726	16.2	(1.0)	0.387	0.607	0.706	16
0.90	0.310	0.582	0.763	16	0.95	0.360	0.606	0.724	16

[a] Parentheses indicate parameters constrained to the indicated values. Left-hand columns: fits to all points. Right-hand columns: fits excluding D_{ch} from the 4.9 MDa PIB solutions, which uniquely used 318-Å spheres as the probe. rmse = fractional root mean square error, in percent.

uted significantly to QELS spectra. So long as the probe and matrix molecular masses differed from each other by a factor of 2 or more, it was feasible to use Laplace inversion to resolve probe and matrix components in the spectrum, thereby determining probe and matrix diffusion coefficients D_{ch} and D_m. The probe species was always dilute, while the concentration c of the matrix species was varied up to the semidilute regime, so D_{ch} was effectively a single-particle (self-) diffusion coefficient, while D_m was a mutual (collective) diffusion coefficient.

Section II of this paper compares D_p of spherical probes with scaling predictions, while section III compares scaling behavior with D_{ch} of polymer probes. Section IV of this paper compares chain and coil diffusion coefficients D in matrix solutions. Discussion and conclusions appear in section V.

II. Spheres in PIB–CHCl$_3$: Scaling Behavior

A previous paper[17] reported D_p of 1595- and 318-Å silica spheres in PIB–CHCl$_3$. Measurements included matrix molecular masses ranging from 57.1 kDa to 4.9 MDa with matrix polymer concentrations as large as 80 g/L. With all sphere:matrix combinations, D_p fell monotonically with increasing c. In concentrated solutions of the higher molecular mass polymers, D_p fell to as little as 0.2% of its value in pure CHCl$_3$. The 318-Å spheres (D_p in pure CHCl$_3$ = 12.68×10^{-12} m^2/s) were used as probes with the 4.9 MDa PIB. For matrix polymers of lower molecular mass (57.1 kDa to 1.9 MDa), the probe species was the 1595-Å spheres (D_p in pure CHCl$_3$ = 2.51×10^{-12} m^2/s).

Reference 17 noted that D_p of silica spheres in PIB–CHCl$_3$ appeared to scale as c/c^*. Once the data were translated along the c axis by distances proportional to the c^* values, a plot of log (D_p/D_0) (where D_0 is D_p as $c \to 0$) against log (c) gave a universal curve. However, in ref 17 a precise form of the universal function was not established, an omission repaired here.

Studies on a wide variety of sphere–polymer–solvent systems have found[22,23] that D_p for spheres in polymer–solvent matrix solutions generally follows a universal scaling law

$$D_p = D_0 \exp(-\alpha c^{\nu}) \qquad (1)$$

Functionally, eq 1 is a stretched-exponential form, whose lack of flexibility limits it to describing functions that depend monotonically on c. Equation 1 can be made consistent with the universal plot observed in ref 17 by rewriting it as

$$\frac{D_p}{D_0} = \exp\left(-\alpha\left(\frac{c}{c^*}\right)^{\nu}\right) \qquad (2)$$

with α now independent of M. Recalling that $c^* \sim M^{-\gamma}c^0$ with $\gamma = 0.5$ in a Θ solvent and $\gamma \approx 0.8$ in a good solvent, a further transformation gives

$$D_p = D_0 \exp(-\alpha(cM^{\gamma})^{\nu}) \qquad (3)$$

Here α and ν are the scaling prefactor and scaling exponent; the prefactors α of eqs 1–3 are not the same. α is in part determined by the units of c and M: here the concentration is given in grams/liter; in eq 3 the molecular mass is in MDa.

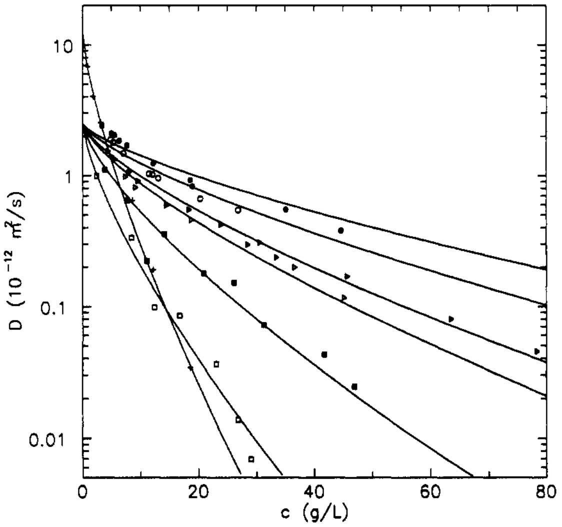

Figure 1. D_{ch} of silica spheres in PIB–CHCl$_3$ solutions plotted against matrix concentration for matrix molecular masses M of 57.1 (●), 95 (○), 182 (▲), 247 (△), 610 (■), 1900 (□), and 4900 (+) kDa. Solid lines are $D_p = D_0 \exp(-0.360(cM^{0.584})^{0.726})$, D_0 referring to spheres in pure CHCl$_3$, for M in MDa.

To determine if eq 3 is an appropriate scaling function for the probe diffusion measurements, nonlinear least-squares fits of eq 3 were made to D_p/D_0. Results of all fits appear in Table I. Numbers in parentheses represent variables that were constrained rather than being used as fitting parameters. To check for possible artifacts due to use of two probe sizes, we made fits both to the complete data set and to the subset having $M \leq 2$ MDa; the subset includes only diffusion measurements made with the larger probe. Exclusion of data on solutions of the 4.9 MDa PIB had virtually no effect on the fits.

Figure 1 shows (solid lines) how well eq 3 with a single trio of fitting parameters (α, γ, ν) can simultaneously describe D_p for solutions with a range of matrix M. Best values for the fitting parameters were $\alpha = 0.360$, $\gamma = 0.584$, and $\nu = 0.726$. As seen in Figure 1, the universal scaling equation (3) with a single set of parameters gives a good account of measurements made at every M.

Because the observed viscosity satisfied $[\eta] \sim 1/c^* \sim M^{0.55}$, the best-fit parameters and the curves in Figure 1 do not give exact compliance of the data with c/c^* scaling. Scaling with c/c^* requires $\gamma = 0.55$. To test for c/c^* scaling, we fit the data to eq 3 with $\gamma = 0.55$ forced, finding $\nu = 0.753$ and $\alpha = 0.33$. The root-mean-square errors (rmse) in fits with γ as a free parameter and with γ fixed at 0.55 were 16 and 17.2%, respectively, so the data are entirely

Table II
Fits to Data of Figure 1, One Matrix Molecular Mass M at a Time, Demonstrating How $D_{\text{ch}} = D_0 \exp(-\alpha c^{\nu})$ Matches with Single-Molecular-Mass Curves[a]

M (kDa)	D_0	α	ν	% rmse	D_0	α	ν	% rmse
57.1	(2.509)	0.077	0.85	11	7.2	0.66	0.40	4
95.1	(2.509)	0.115	0.80	8	106	3.1	0.16	1
182	(2.509)	0.209	0.68	4	2.36	0.188	0.697	3.6
247	(2.509)	0.241	0.66	8	3.00	0.325	0.596	8
610	(2.509)	0.317	0.69	11	2.22	0.267	0.73	11
1900	(2.509)	0.41	0.78	27	1.78	0.279	0.877	27
4900	(12.68)	0.64	0.64	13	8.65	0.406	0.89	9.9

[a] Parentheses denote parameters constrained to the indicated values. Left- and right-hand groups of columns refer to D_0 constrained to its pure-solvent value or treated as a free parameter, respectively. c in g/L; D_0 in 10^{-7} cm^2 s^{-1}.

consistent with the simple form

$$\frac{D_{\text{p}}}{D_0} = \exp\left(-\alpha'\left(\frac{c}{c^*}\right)^{3/4}\right) \tag{4}$$

In studies of chain probes (polystyrenes) in PVME–o-fluorotoluene, Wheeler et al.[12,13] noted that using D_0 as a free parameter substantially improved agreement between eq 1 and their probe data. Wheeler et al. found that their best-fit values of D_0 were substantially larger than the true low-concentration value of D. With our measurements, taking D_0 as a free parameter gives values for $D(c)$ that are 5–10% smaller, not larger, than the correct value. However, removing the constraint on D_0 has almost no effect on the rmse in the fit, so our measurements are entirely consistent with an identification of D_0 as the true zero-concentration limit of D_{p}. The behavior of the unconstrained D_0 observed by Wheeler et al. can reasonably be interpreted as arising from contraction of their random-coil probes at elevated c.[12,13] Our silica probes do not contract at elevated matrix concentrations, so we expect silica probes to lack the D_0 behavior treated by Wheeler et al.; Table I is in complete agreement with our expectation.

Careful inspection of Figure 1 suggests that D_{p} may not be precisely a function of c/c^*. For the larger-M matrices, the scatter of points around the solid lines appears random. For the lowest-molecular-mass matrices (M = 57.1 and 95.1 kDa), deviations between the data and the fit lines appear systematic, the predicted D_{p} consistently being too small at low c and too large at high c.

To examine the extent of the dependence of D_{p}/D_0 on M, data for each matrix molecular mass were separately fit to eq 1, gaining results summarized in Table II. Most of the individual fits are much better (rmse of 4–13%) than was the collective fit of data for all seven M values to eq 3. Table II shows results obtained on constraining D_0 to the value of D_{p} in pure solvent and results obtained by treating D_0 as a free parameter. With D_0 constrained, α increases smoothly with increasing M, while ν tends to decrease. With D_0 free, all three fitting parameters show an irregular, scattered correlation with M; the eight to ten measurements of D_{p} taken at a single M are simply inadequate to determine three nonlinearly coupled parameters simultaneously. We conclude that the fits in Table II made with D_0 constrained are to be preferred to fits made with D_0 free.

As seen in Figure 2, with D_0 constrained α exhibits a progressive increase with increasing M. For these fits, ν is in the range 0.72 ± 0.1. For the observed molecular mass range, there is an 8-fold increase in α consequent to an 80-fold increase in M, which corresponds roughly to $\alpha \sim M^{1/2}$, the proportionality implied by Table I. Except for solutions of the 1.9×10^6 Da polymer, results for which are fit poorly by eq 1, ν does fall slightly with increasing M, contrary to the assumption in eq 1 that ν is independent of M. From Table II, we conclude that eq 3 is a good first approximation but that careful examination reveals weak systematic deviations of $D_{\text{p}}(c,M)$ from a universal functional behavior.

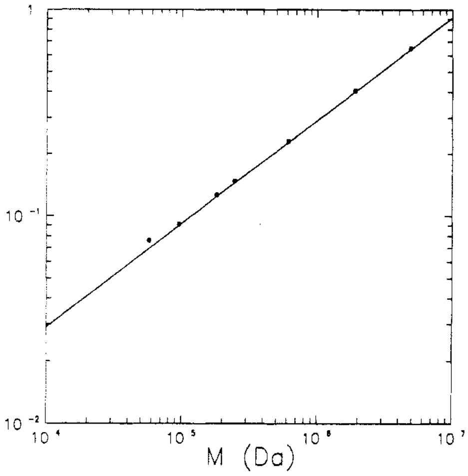

Figure 2. α from fits of $D_{\text{p}} = D_0 \exp(-\alpha c^{\nu})$ to $D_{\text{p}}(c)$ for silica spheres in PIB solutions of concentration c with PIB of molecular mass M, D_0 being the pure-solvent value. Solid line is $\alpha \sim M^{1/2}$.

III. Random Coils in PIB–CHCl$_3$: Scaling Behavior

Previous papers[16,17] report on diffusion by dilute polyisobutylenes through PIB solutions. The experiments were done using quasi-elastic light scattering. Mixtures containing two species of PIB of different molecular mass were examined; D_{ch} of a dilute species is that species' single-chain diffusion coefficient in the mixture. The experimental method precludes measurement of true self-diffusion coefficients for a single species.

Figures 3 and 4 present D_{ch} for small probe chains diffusing through large (4.9×10^6 and 1.1×10^6 Da, respectively) matrices. Denoting probe and matrix molecular masses by P and M, respectively, in the former figure, $P < M$ always obtains; the latter figure includes results for $P > M$ and also $P < M$. Figure 5 shows D_{ch} for large probe chains ($P = 4.9 \times 10^6$ Da) diffusing through low-M matrix chains. Tables III and IV summarize fits of D_{ch} to eq 1 for a range of P and M. Table III presents results on small probes (P in the range 182–100 kDa) diffusing through large-M matrices (4.9 and 1.1 MDa), while Table IV describes D_{ch} for large probes ($P \geq 1.9$ MDa) diffusing through low-M (80–1100 kDa) matrices.

Fits were made both with D_0 constrained to its dilute-solution limit and with D_0 as a free parameter. From the tables, using D_0 as a free parameter generally does not improve the quality of the fit. In addition to the fits shown in the tables, in which ν was retained as a free parameter, we tested the possibilities ν = 1.0 (exponential concen-

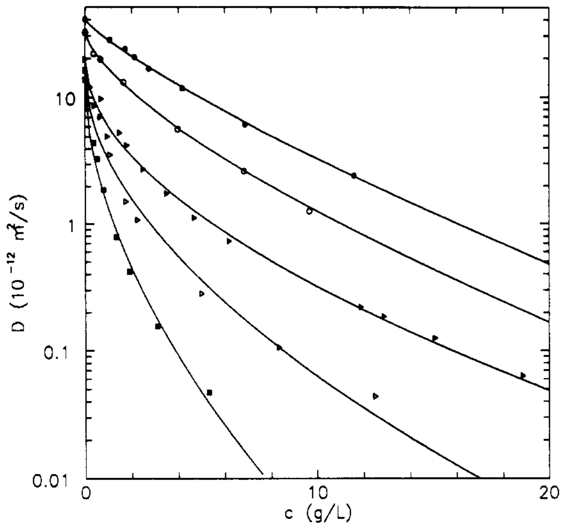

Figure 3. D_{ch} of low-molecular-mass probes (P = 182 (●), 247 (○), 610 (▲), 856 (△), and 1100 (■) kDa) in CHCl$_3$–4900 kDa PIB. Solid lines are fits to eq 1 with α and ν as free parameters.

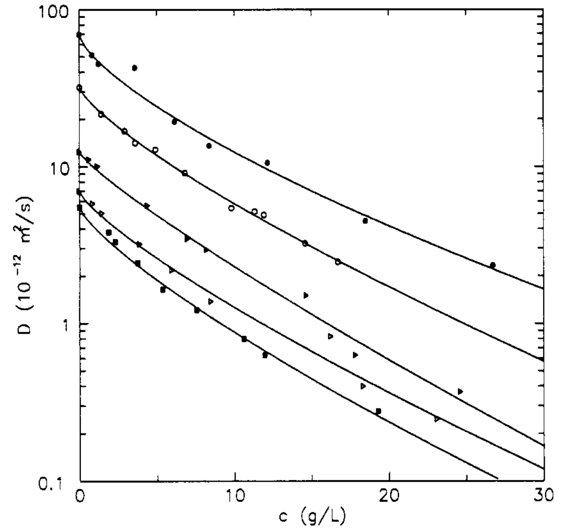

Figure 4. D_{ch} of small (P = 80 (●) and 247 (○) kDa) and large (P = 1900 (▲), 3800 (△), and 4900 (■) kDa) probe chains in CHCl$_3$–1100 kDa PIB. Solid lines are from fits to eq 1 with α and ν as free parameters.

tration dependence) and $\nu = {}^1/_2$ by making fits with ν constrained to one of these two values. In a few systems in which the best fit ν is 0.55, forcing $\nu = 0.5$ does not degrade the fit especially. In all other cases, constraining ν to 1.0 or 0.5 greatly increases the % rmse, typically by a factor of 2 or 3. The following remarks are therefore limited to systems in which D_0 was constrained while ν was adjusted to improve the fit.

For small probes and the largest matrix (Table III), α increases substantially with increasing P, a 6-fold increase in P being accompanied by a 6-fold increase in α. In the same small probe–large matrix systems, α depends modestly on M: with P = 247 kDa, increasing M from 1.1 to 4.9 MDa barely doubles α (from 0.28 to 0.65). On the other hand (Table IV), for large probes and low-molecular-mass matrix polymers, α depends only weakly on M; with P = 4.9 MDa, increasing M from 80 to 1100 kDa barely doubles α (from 0.16 to 0.31). In large molecular mass probe–small matrix systems, α depends at most weakly on P; with M = 1100 kDa, reducing P from 4.9 to 1.9 MDa only reduces α from 0.31 to 0.24. Except for very large probes in solutions of the largest matrix, where ν is roughly ${}^1/_2$, we find consistently ν to be about ${}^3/_4$, with no indication of an appreciable dependence of ν on P or M.

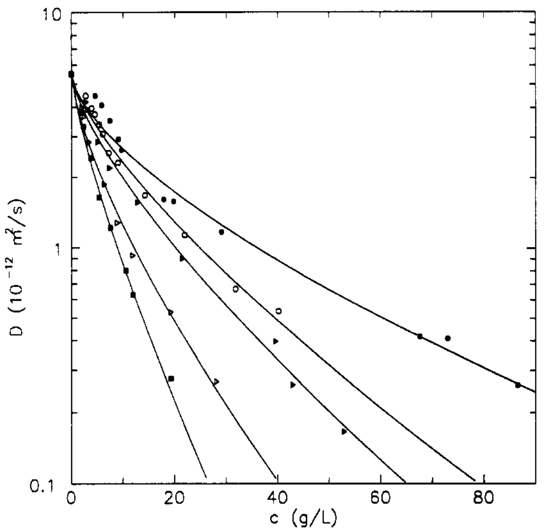

Figure 5. D_{ch} of large (P = 4.9 MDa) probe chains in matrix solutions with M of 80 (●), 182 (○), 247 (▲), 610 (△), and 1100 (■) kDa. Solid lines are from fits to eq 1 with α and ν as free parameters.

Equation 1 is a prediction of the hydrodynamic scaling model for polymer self-diffusion; observation of a stretched-exponential concentration dependence for D_{ch} provides a mild confirmation of this model. However, the theoretical development that leads to eq 1 is[21] presently limited to $P \approx M$. The above values for α and ν in systems having $M \neq P$, and the dependences of α and ν on M and P, are presently a guide for further developments but are not yet useful tests of the model.

IV. Chains and Sphere Diffusion

Figures 6 and 7 compare diffusion of spherical and random-coil probe particles in PIB–CHCl$_3$.[16] These figures comprise a definitive test of the relative merits of hydrodynamic scaling and entanglement models for polymer solution dynamics. Figure 6 gives D for 1595-Å silica spheres and 4.9×10^6 Da PIB chains in matrix solutions containing 6.1×10^5 Da PIB chains, while Figure 7 gives D of 318-Å silica spheres and 1.1×10^6 Da PIB chains in solutions of 4.9×10^6 Da PIB chains. In both figures, the $c \rightarrow 0$ limits of D_p and D_{ch} are relatively close to each other. In each figure, a comparison is made between probes of different architectures whose translational motions occur on nearly the same time scale. In each figure D (i.e., D_p or D_{ch}) falls substantially with increasing matrix c, D/D_0 of less than 0.1 (in the low-M matrix) or 0.01 (in the large-M matrix) being observed.

Figure 6 compares random-coil and spherical probes having similar hydrodynamic radii ($D_0 = 5.5 \times 10^{-12}$ and 2.51×10^{-12} m^2/s, respectively) diffusing through solutions of a small, rapidly-diffusing ($D_0 = 19.7 \times 10^{-12}$ m^2/s) matrix polymer. The matrix polymer has $c^* = 1/[\eta]$ of 9.3 g/L, so Figure 6 covers both dilute and semidilute ($0 \leq c/c^* \leq 3.0$) concentrations. Over the entire range (0–30 g/L) of matrix concentrations, D_p/D_{ch} of the two probe species remains virtually constant, the chains consistently diffusing slightly more than twice as fast as the spheres.

Figure 7 again compares diffusion of sphere and random-coil probe molecules, this time in solutions containing a matrix polymer that is somewhat larger than either of the probe species. The infinite-dilution limiting diffusion coefficients of the probe (P), sphere (S), and matrix (M) species are 13.7×10^{-12}, 12.7×10^{-12}, and 5.5×10^{-12} m^2/s, respectively, so the hydrodynamic radii of the two probe species are within 10% of each other and are ≈40% of the

Table III
Diffusion[a] of Small Probes (Molecular Mass P) through Large Matrices (Molecular Mass M) As Described by $D_{ch} = D_0 \exp(-\alpha c^{\nu})$

M (kDa)	P (kDa)	D_0	α	ν	% rmse	D_0	α	ν	% rmse
4900	182	(40.2)	0.369	0.83	3	41	0.383	0.82	3
4900	247	(31.88)	0.645	0.707	3.1	31.0	0.620	0.722	2.9
4900	610	(19.7)	1.19	0.54	11.7	21.5	1.26	0.52	11.3
4900	856	(16.2)	1.60	0.54	27	19.8	1.77	0.51	26
4900	1100	(13.69)	2.34	0.55	16	14.84	2.92	0.54	15.7
1900	247	(31.88)	0.368	0.767	7.3	32.96	0.388	0.752	7.2
1100	80	(69.4)	0.340	0.705	12	70.4	0.348	0.699	12
1100	247	(31.9)	0.283	0.78	5	31.57	0.277	0.786	5

[a] Left-hand columns refer to fits with D_0 constrained to its pure-solvent value; right-hand columns refer to D_0 used as a free parameter. Parentheses denote parameters constrained to the indicated values. c in g/L; D_0 in 10^{-7} cm^2 s^{-1}.

Table IV
Diffusion[a] of Large Probes (Molecular Mass P) through Small Matrices (Molecular Mass M) As Described by $D_{ch} = D_0 \exp(-\alpha c^{\nu})$

M (kDa)	P (kDa)	D_0	α	ν	% rmse	D_0	α	ν	% rmse
80	4900	(5.5)	0.16	0.66	12.6	23.8	1.00	0.33	6.4
182	4900	(5.5)	0.157	0.77	8.1	12.4	0.64	0.43	3.9
247	4900	(5.5)	0.190	0.73	9.4	6.9	0.29	0.64	8.8
610	4900	(5.5)	0.29	0.71	9.8	12.8	0.85	0.45	3.2
1100	4900	(5.5)	0.31	0.78	7.4	10.1	0.70	0.55	2.8
1100	1900	(12.42)	0.237	0.853	12	13.0	0.260	0.829	12
1100	3800	(6.96)	0.277	0.79	13	7.22	0.296	0.77	12.9
1100	4900	(5.5)	0.307	0.777	6.9	5.8	0.337	0.75	6.5

[a] Left-hand columns refer to fits with D_0 constrained to its pure-solvent value; right-hand columns refer to D_0 used as a free parameter. Parentheses denote parameters constrained to the indicated values. c in g/L; D_0 in 10^{-7} cm^2 s^{-1}.

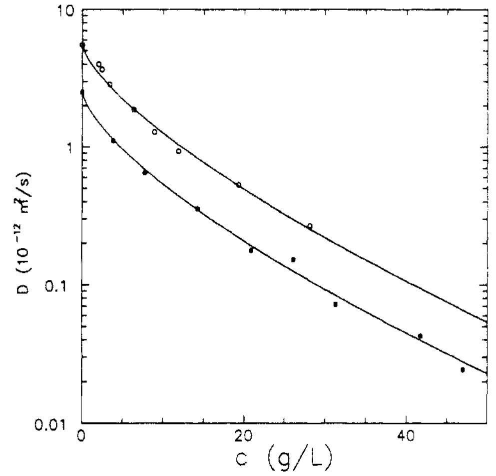

Figure 6. Diffusion coefficients of 1595-Å silica spheres (filled circles) and 4.9×10^6 Da polyisobutylene (open circles) through 6.1×10^5 Da polyisobutylene–$CHCl_3$ plotted against matrix c. For large probes ($D_0 = 2.51 \times 10^{-12}$, 5.5×10^{-12} m^2/s, respectively) in solutions of a small ($D_0 = 19.7 \times 10^{-12}$ m^2/s) matrix, the fractional degree of retardation of the probes is manifestly independent of probe architecture.

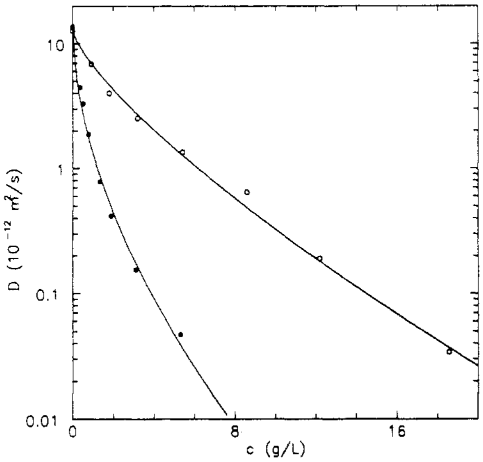

Figure 7. Diffusion coefficients of 318-Å silica spheres (open circles) and 1.1×10^6 Da PIB (filled circles) through 4.9×10^6 Da polyisobutylene–$CHCl_3$ plotted against matrix c. In contrast to Figure 6, for small probes ($D_0 = 13.7 \times 10^{-12}$, 12.7×10^{-12} m^2/s, respectively) in solutions of a large ($D_0 = 5.5 \times 10^{-12}$ m^2/s) matrix, the retardation of the probes depends strongly on probe architecture, random coils being retarded more strongly than rigid spheres, contrary to expectations from tube-type models but consistent with hydrodynamic scaling.

radius of a matrix polymer. For 4.9 MDa polyisobutylene, $c^* = 1/[\eta] \approx 3$ g/L, so D_{ch} was obtained for c up to $2c^*$ while D_p was obtained for c up to $6c^*$. From Figure 7, increasing c from 0 to 5 g/L reduces the spheres' D_p by roughly 10-fold but reduces D_{ch} of the probe chains by more than a 100-fold. A very-high-molecular mass matrix polymer is therefore far more effective at retarding diffusion by a random coil than at retarding diffusion by a solid sphere of equal size.

Figure 7 represents conditions optimal for observing the diffusion of reptational behavior:

First, the matrix M is extremely large (4.9×10^6 Da), larger than almost all other data in the literature. The probe chains, while large ($P = 1.1 \times 10^6$), are much smaller than the matrix. Relative molecular masses of the probe and matrix polymers satisfy $P/M \leq 0.23$. It has previously been found[24] that D_{ch} of chains in chain melts becomes independent of M (i.e., D_{ch} shows scaling-law $P^{-2}M^0$ behavior) only if P/M is sufficiently small; the system represented in Figure 7 is in this small P/M limit. This system therefore is in the molecular mass regime where reptation would be expected to be important. (One can always claim that an M, however large, is too small to exhibit entangled behavior. However, if 4.9 MDa is too small for entanglements to be important, then entanglements are not significant for the systems treated in virtually the entirety of the published literature on polymer solutions, because almost all of this literature treats polymers smaller than 1 MDa.)

Second, the concentration regimes included here are appropriate for a study of reptation. c and c^* are sufficiently small that "monomer friction" issues should not be significant. From viscoelastic determinations[25] polyisobutylene has an entanglement molecular weight $M_E \approx 7600$, so in this system $c_E \approx \rho M_E/M \leq 2$ g/L. While it is often true that $c_E \gg c^*$, polyisobutylene is rather unusual in having $c_E \approx c^*$, perhaps because it is unusually lacking in stiffness. We therefore determined both D_p and D_{ch} in the overlapping, entangled regime $c > c^*$, c_E.

Tube-type models make clear predictions as to the relative self-diffusion coefficients of large chains and equally large spheres in entangled polymer solutions. A rigid spherical body is limited to Stokes–Einstein type diffusion; a rigid sphere cannot reptate. It is often assumed, e.g., ref 1, that Stokes–Einstein diffusion is necessarily determined by the macroscopic zero-shear, zero-frequency viscosity η_0 of the solution, though it is not clear from the usually-invoked arguments that Brownian motion (which is neither straight line nor constant in velocity) could not be sensitive to a frequency dependence of η or other rheological properties.

In contrast to rigid spheres, which only perform Stokes–Einstein diffusion, random-coil chains can perform both Stokes–Einstein diffusion and reptation. Since Stokes–Einstein and reptational modes are independent, their contributions to D are nearly additive. In entangled solutions ($c > c^*$, M and P large enough that matrix chains entangle both themselves and probe chains), Stokes–Einstein diffusion by chains should be very slow, so reptation will dominate Stokes–Einstein diffusion when both are present. For spherical and random-coil probes of equal size, diffusing in semidilute solutions of a large polymer, tube-type models thus predict $D_{ch} \gg D_p$, the ratio D_{ch}/D_p increasing with increasing c. Invoking this argument, Numasawa et al.[26] used a variable $X = 6\pi\eta R_g D/(k_B T)$ to separate diffusive behaviors of polystyrene chains in poly(methyl methacrylate)–benzene into a nominal Stokes–Einstein regime ($X \approx 1$) and a nominal reptational regime ($X \gg 1$).

Figure 7 conclusively rejects conventional tube-type ("reptational") models for polymer dynamics. Despite circumstances optimal for the observation of reptational behavior, we find $D_{ch} \ll D_p$, not the $D_{ch} \gg D_p$ demanded by entanglement pictures of polymers in solution. In our measurements, at all c the functional fit to $D_{ch}(c)$ lies far below the corresponding fit to $D_p(c)$. While we only measured D_{ch} out to $2c_E$, our data strongly imply that $D_{ch} \ll D_p$ far into the entangled regime. That is, D_{ch} at 5 g/L is roughly equal to D_p at 18 g/L. To obtain the reptation prediction $D_{ch} \gg D_p$ at 18 g/L (18 g/L $\approx 6c_E$, well into the entangled regime), between 6 and 18 g/L it would be necessary for D_{ch} to increase substantially with increasing matrix c. An increase in D_{ch} with increasing c is contrary to all experience, which uniformly shows that D_{ch} decreases monotonically with increasing c. (It should be recalled that the hydrodynamic scaling model places nominally dilute and nominally semidilute solutions on the same footing, so the locations of c^* and c_E are not significant in tests of hydrodynamic scaling.)

Even under the very favorable experimental conditions used to generate Figure 7, polymer chains clearly do not have additional modes of motion in excess of the modes of motion accessible to rigid spheres. Our results do not preclude the existence of a novel chain mode that is so highly anticorrelated with Stokes–Einstein diffusion that chain and Stokes–Einstein displacements tend to cancel, but to our knowledge no model predicts such a mode.

The above argument noted Numasawa et al.'s[26] classification of chain diffusion. It is fair to recall that Numasawa et al. only report data on random-coil probes. Numasawa et al.'s experimental data are consistent with ours. Their identification of a "reptational" regime follows from the understandable assumption that large increases in $D\eta$ over its $c = 0$ value could only follow from the introduction of new, non-viscosity-limited modes of chain motion, an assumption not consistent with results on D_p in concentrated polymer solutions.[22]

V. Discussion and Conclusions

In conclusion, we have reexamined measurements of sphere and coil diffusion through PIB–CHCl$_3$ solutions. We find that D_p of spherical probe particles has a stretched-exponential dependence on the scaling variable c/c^*; equivalently, we find $\alpha \sim M^{1/2}$. The concentration scaling exponent ν for this form is very nearly $^3/_4$, a value central to the range (1.0, 0.5) previously observed[22,23] for ν. For the diffusion of random-coil chains through PIB solutions, we find that D_{ch} of the probe chains has a stretched-exponential dependence on the matrix concentration, with a scaling exponent $\nu \approx {}^3/_4$. For $P \ll M$, α depends substantially on P and less on M. For $P \gg M$, α depends relatively weakly on either P or M. The concentration dependence of D_{ch} is consistent with the hydrodynamic scaling model,[21] at least within the limits on current deviations of that model.

D of spherical and probe particles moving through the same matrix has been examined. *Under circumstances highly favorable for observing reptational modes, we find that such modes are clearly not significant*; random coils move less quickly than rigid spheres through solutions of large chains, contrary to entanglement pictures. The observed relationships between D_p and D_{ch} presented here are, however, consistent with the hydrodynamic scaling model of polymer dynamics.

A further semiquantitative test of the hydrodynamic scaling model is obtained by comparing values of the interaction parameter α for probe spheres and probe chains. α of eq 1 has the dependences

$$\alpha \sim \frac{R_p R_m^{\,3}}{aM} \qquad (5)$$

Here R_p and R_m are the radii of the probe and matrix chains and a is a distance of closest approach between hydrodynamic units of the probe and matrix. The model neglects intrachain motions, which is clearly inappropriate if the probe and matrix differ greatly in size, because the (excluded) intrachain motions of a large body can involve the same time scale as the (included) translational motions of the small body.

If the probe is a large sphere, $a \approx R_p$, because the distance of closest approach of a large hard sphere and a polymer bead is $R_p + a_0 \approx R_p$, a_0 being a bead radius. Since $c^* \sim M/R_m^{\,3} \sim M^{\gamma}$, one has

$$\alpha \sim R_p^{\,0} R_m^{\,3}/M \sim 1/c^* \qquad (6)$$

For large spheres diffusing through chains of roughly the same radius, the hydrodynamic scaling model thus predicts $\alpha \sim R_p^{\,0}/c^*$. Experimentally, we found eq 3, which is in complete agreement with hydrodynamic scaling: (i) in fits to eq 3, a common value of α was adequate for data on both sphere sizes, confirming $R_p^{\,0}$ behavior of α, and (ii) in these same fits, c appeared as a function of c/c^* or cM^{γ}, confirming the $R_p^{\,3}/M$ behavior of α.

For random-coil chains diffusing through matrix chains, $a \approx 2a_0$. Denote α for a polymer chain and a probe sphere by α_{ch} and α_p, respectively. For a polymer chain and a sphere having the same R_p in the same matrix, eqs 5 and

6 indicate

$$\frac{\alpha_{ch}}{\alpha_p} = \frac{R_p}{\alpha} \qquad (7)$$

In the regime in which the hydrodynamic scaling model is valid, α for coils should be substantially larger than α for spheres. Figure 7 confirms qualitatively this expectation of the hydrodynamic scaling model; for the data in the Figure, $\alpha_p/\alpha_{ch} \approx 4$. Equation 7 will break down if the probe and matrix molecules become sufficiently different in size, as is apparently the case in Figure 6.

It has long been known[22] that the Stokes–Einstein equation fails for large globular probes in polymer solutions, the product $D\eta$ rising above its value in pure solvent. For probes and chains in lower-M solutions a weak failure of Stokes–Einstein behavior is observed,[17] $D\eta$ increasing at large c both for chains and for spheres. At large M, Figure 7 implies that Stokes–Einstein failures for chain and globular probes are not the same; however, we lack viscosity information for this system.

References and Notes

(1) de Gennes, P.-G. *Scaling Concepts in Polymer Physics*; Cornell University Press: Ithaca, NY, 1979, 1988.
(2) Doi, M.; Edwards, S. F. *The Theory of Polymer Dynamics*; Clarendon Press: Oxford, 1986.
(3) Phillies, G. D. J. *Macromolecules* **1986**, *19*, 2367.
(4) Phillies, G. D. J. *J. Phys. Chem.* **1989**, *93*, 5029.
(5) Leger, L.; Hervet, H.; Rondelez, F. *Macromolecules* **1981**, *14*, 1732.
(6) Lodge, T. P.; Rotstein, N. A.; Prager, S. *Adv. Chem. Phys.* **1990**, *79*, 1.
(7) (a) Grest, G. S.; Kremer, K. *Springer Proceedings in Physics*; *Computer Simulation Studies in Condensed Matter Physics*; Landau, D. P., Mon, K. K., Schuettler, H. R., Eds.; Springer-Verlag: Berlin, 1988; Vol. 33, pp 76–83. (b) Kremer, K.; Grest, G. S. *J. Chem. Phys.* **1990**, *92*, 5057.
(8) Kolinski, A.; Skolnick, J.; Yaris, R. *J. Chem. Phys.* **1987**, *86*, 1567, *86*, 7164, 7174.
(9) Hess, W. *Macromolecules* **1986**, *19*, 1395; **1988**, *21*, 2620.
(10) Oono, Y.; Baldwin, P. R. *Phys. Rev.* **1986**, *A33*, 3391.
(11) Ngai, K. L.; Rendell, R. N.; Rajagopal, S. T. *Ann. N.Y. Acad. Sci.* **1984**, *484*, 150.
(12) Wheeler, L. W.; Lodge, T. P. *Macromolecules* **1989**, *22*, 3399.
(13) Lodge, T. P.; Markland, P.; Wheeler, L. W. *Macromolecules* **1989**, *22*, 3409.
(14) Phillies, G. D. J. *Macromolecules* **1990**, *23*, 2742.
(15) Phillies, G. D. J. *J. Non-Cryst. Solids* **1991**, *131-133*, 612.
(16) Brown, W.; Zhou, P. *Macromolecules* **1989**, *22*, 4031.
(17) Zhou, P.; Brown, W. *Macromolecules* **1989**, *22*, 890.
(18) Brown, W.; Zhou, P. *Polymer* **1990**, *31*, 772.
(19) Livesay, A. K.; Licinio, P.; Delaye, M. *J. Chem. Phys.* **1986**, *84*, 5102.
(20) Licinio, P.; Delaye, M.; Livesay, A. K.; Leger, L. *J. Phys. (Les Ulis, Fr.)* **1987**, *48*, 1217.
(21) Phillies, G. D. J. *Macromolecules* **1987**, *20*, 558.
(22) Phillies, G. D. J.; Ullmann, G. S.; Ullmann, K.; Lin, T.-H. *J. Chem. Phys.* **1985**, *82*, 5242.
(23) Phillies, G. D. J.; Gong, J.; Li, L.; Rau, A.; Zhang, K.; Yu, L.-P.; Rollings, J. *J. Phys. Chem.* **1989**, *93*, 6219.
(24) Sillescu, H. J. *J. Non-Cryst. Solids* **1991**, *131-135*, 593.
(25) Ferry, J. D. *Viscoelastic Properties of Polymers*; John Wiley: New York, 1980; p 374.
(26) Numasawa, N.; Kuwamoto, K.; Nose, T. *Macromolecules* **1986**, *19*, 2593.

Registry No. PIB, 9003-27-4; $CHCl_3$, 67-66-3; SiO_2, 7631-86-9.